6 Non-radiative recombination

Luminescence efficiency or quantum yield almost never reaches $\eta = 1$; even if this were the case, Stokes' law implies that a portion of the supplied excitation energy is not transformed into luminescence radiation but, during relaxation to the system ground state, changes into other types of energy instead. The relevant transitions are called *non-radiative transitions* and the relevant electron–hole recombination is called *non-radiative recombination*. It is mostly an undesirable competing effect, which can even result, under strong pumping, in local overheating and mechanical damage of the material.

Depending on the final form of the dissipated excitation energy, one can recognize three basic types of non-radiative recombination in semiconductors:

1. recombination when the excitation energy transforms into heat (phonons);
2. recombination leading to a creation of new point defects in the lattice;
3. recombination transforming the excitation energy into photochemical changes of the material under study.

The first type of non-radiative recombination, which consequently slightly increases the sample temperature, is found most commonly. Within its framework, multiphonon transitions and Auger recombination can be distinguished. Photochemical changes induced by excitation radiation are restricted to only a limited number of compounds such as halides of silver and thallium. Similarly, the formation of lattice defects occurs quite rarely, mainly in some wide-bandgap materials at the border between semiconductors and ionic crystals.

Even though the theoretical foundations of non-radiative recombination processes in semiconductors are covered in the monograph by Abakumov *et al.* [1], in general non-radiative recombination is not as widely studied and understood as the diverse types of radiative recombination.

6.1 Transformation of the excitation energy into heat

6.1.1 Multiphonon recombination

The simplest idea that comes to mind under the concept of 'multiphonon non-radiative recombination in semiconductors' is probably as follows: an excited electron near the bottom of the conduction band, a hole near the valence band maximum and the entire excitation energy is—instead of being emitted in the form of photons $h\nu \cong E_g$ owing to radiative e–h recombination—handed over to the lattice through n phonons with energy $\hbar\omega$: $E_g = n\hbar\omega$, as depicted in Fig. 6.1(a). Actually, it is a non-radiative analogy of bimolecular recombination, discussed in Section 3.3. However, this process is highly improbable. From the perturbation theory point of view, it is an nth order process and for its probability $1/\tau_{nr}$ a relation like $1/\tau_{nr} \approx \exp(-E_g/\hbar\omega) \approx \exp(-n)$ can be foreseen. For a typical semiconductor with $E_g \approx 2$ eV and $\hbar\omega \approx 25$ meV we obtain $n = 80$, therefore, the corresponding probability is negligibly small and decreases with increasing forbidden gap E_g. Moreover, expression (5-9b) implies that the probability of the radiative transition, considering its proportion to ν^2, increases strongly in this case with the value of $h\nu(\approx E_g)$. Therefore, there are two reasons why wide-bandgap semiconductors outperform, as far as the luminescence efficiency is concerned, those with a narrow bandgap.

The probability of such free electron–hole pair non-radiative bimolecular recombination would increase substantially if a deep energy level occurs

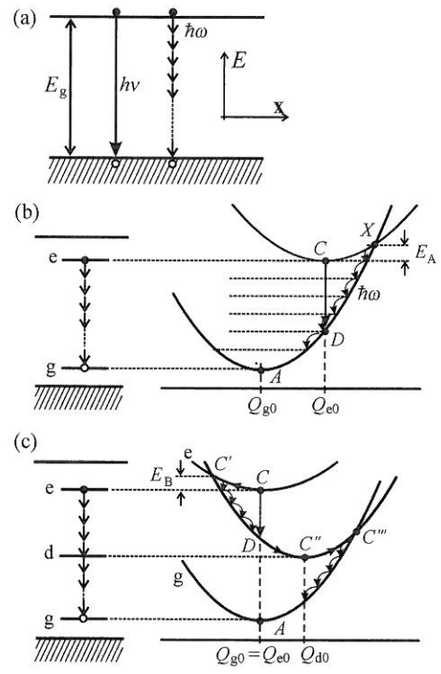

Fig. 6.1
(a) Non-radiative bimolecular recombination of free electron–hole pairs across the bandgap via multiple phonon $\hbar\omega$ emission. This process in fact does not occur in reality. (b) Non-radiative transition in a localized luminescence centre $C \to X \to A$ through the emission of many local phonons $\hbar\omega$('cooling transitions'). The centre is assumed to be in strong interaction with the lattice (high local change in the coordinate Q_{e0}–Q_{g0}). (c) Non-radiative transition into the ground electronic state $C \to C' \to C'' \to C''' \to A$ inside a localized centre that has only a weak interaction with the lattice ($Q_{e0} \approx Q_{g0}$). The non-radiative recombination is mediated by a deep level d. The thermal activation energy of the transition is denoted by E_B.

approximately in the middle of the bandgap; this process will be discussed in the next subsection. Now we shall pay attention to how non-radiative multiphonon transitions can be applied in a *localized luminescence centre*. Actually, we have already addressed the problem for the case of strong exciton–phonon coupling in Section 4.6, with the help of Fig. 4.8(b); its salient features are reproduced here as Fig. 6.1(b). The ordinate of the intersection point X lowers with increasing difference $Q_{g0} - Q_{e0}$ (i.e. with increasing exciton–phonon binding) and so does the activation energy E_A. The excited centre then reaches point X easily and then, down the trajectory $X \rightarrow A$, it may pass non-radiatively to the ground electronic state, emitting local phonons. Notice that the phonon emission here has a character substantially different from the (hypothetical) non-radiative bimolecular recombination depicted in Fig. 6.1(a). While in Fig. 6.1(a) multiphonon emission would be mediated by 'virtual' electron levels (much like, for instance, two-photon absorption) and therefore it would be a pure process of nth order perturbation theory, in the case of a localized centre, on the other hand, it proceeds by sequential application of one-phonon processes with participation of a real intermediate level.[1] The probability of such processes is then incommensurately higher, and non-radiative recombination of the localized centre via local phonon emission becomes very efficient, provided the centre is in strong enough interaction with the lattice.

If the localized centre interacts with the surrounding lattice only very weakly (e.g. rare earth ions), then $Q_{g0} \approx Q_{e0}$ (Fig. 6.1(c)) and the point of intersection X in fact does not exist. In this case, non-radiative recombination with many-phonon emission also becomes improbable, similarly to the case of a free electron–hole pair depicted in Fig. 6.1(a). Apart from other things this is one of the reasons why rare earth ions represent efficient luminescent centres if embedded into any lattice, as we have already discussed in Section 5.6.

Here, a very important factor mediating non-radiative recombination proves to be a *deep level* lying approximately in the middle of the bandgap, which corresponds to a defect located in the vicinity of the luminescent centre. It is significant that a defect associated microscopically with the deep level is always in strong interaction with the surrounding lattice, therefore the configurational coordinate changes from Q_{e0} to Q_{d0} during transfer of the excitation energy to this defect (Fig. 6.1(c)). This allows for a gradual dissipation of the electron excitation energy via 'cooling transitions' $C \rightarrow C' \rightarrow C''$. From here, the remaining energy 'spills' into the matrix by a pathway of similar character $C'' \rightarrow C''' \rightarrow A$, thus completing the non-radiative relaxation of the excited luminescence centre via multiphonon emission. The non-radiative recombination mediated by a defect is sometimes called Shockley–Read recombination.

It is worth realizing that, at the same time, the radiative channel of this centre may not be completely blocked ($\tau_r \rightarrow \infty$). The transition $C \rightarrow D$ in Figs 6.1(b) and 6.1(c) comprises the emission of a luminescence photon; transitions to the deep level can therefore be accompanied by weak broadband

[1] Such transitions are sometimes called 'cooling transitions' because they lead to a decrease of the non-equilibrium amplitude of the vibrations in the excited electronic state, therefore to a decrease of the high effective temperature.

luminescence. However, the intensity of such luminescence strongly decreases with decreasing thermal activation energy E_B (Fig. 6.1(c))—in other words, the stronger the interaction of the deep defect with the surrounding matrix, the weaker is the luminescence connected with this deep level.

We assumed tacitly that the luminescence centre was photoexcited via a path $A \rightarrow C$, see Fig. 6.1(c). The excitation energy, however, can be supplied to the centre also via capturing injected free carriers (the case of injection electroluminescence). This presumes, however, a sufficient electric conductivity of the surrounding lattice. Luminescence quenching of this type does indeed occur in light-emitting diodes [2].

What is the microscopic basis of the non-radiative centre constituting the deep level? In many cases this is not known precisely. It may be dislocations or vacancies in the bulk of the semiconductor, or recombination in the proximity of the interface between two materials may be involved (dislocations caused by different lattice constants, aggregated impurity atoms). Nevertheless, what is especially worth mentioning is the so-called *surface recombination*.

Surface recombination is a specific non-radiative recombination in solid-state phosphors, which takes place only in a thin subsurface layer and is conditioned by the occurrence of deep localized levels located within the forbidden gap (sometimes called Tamm levels or Tamm surface states). It is known that these levels, related to surface electron states, owe their origin to perturbation of the ideal translation symmetry of the infinite lattice by the crystal surface. More exactly, from the microscopic point of view it is unoccupied (dangling) bonds of surface atoms in a semiconductor that give rise to these levels.

For the sake of simplicity let us assume an intrinsic semiconductor, excited with a generation rate G. The situation is depicted in Fig. 6.2(a). As a consequence of the existence of the deep levels under discussion, the non-radiative recombination (see Fig. 6.1(c) or possibly Fig. 6.5) will be strongly inhomogeneous along the x coordinate normal to the surface, assuming a maximum at $x = 0$. This means, however, that the photocarrier concentration $n(x)$ just under the surface will decrease significantly, thus creating a concentration gradient driving photocarriers to the surface. Kinetic equations describing the generation and recombination processes then will, in comparison with previous considerations, incorporate an additional term arising from the *diffusion current* density $|\mathbf{j}| = -D|\operatorname{grad} n(x)| = -D\partial n(x)/\partial x$, where D stands for the diffusion coefficient of the carriers.[2]

We now analyse a steady-state regime, i.e. we apply the kinetic equations for $\partial/\partial t = 0$. The diffusion term, containing a derivative with respect to the space coordinate x, thus enters the kinetic equations through Fick's second law in the form of $-\partial/\partial x(-D\partial n(x)/\partial x)$. Thus instead of equation of the type (3.4) we have

$$D\,\frac{\mathrm{d}^2 n(x)}{\mathrm{d}x^2} - \frac{n(x)}{\tau} = -G, \tag{6.1}$$

[2] Carrier diffusion is in this case governed by slower (heavier) carriers which, via Coulomb interaction, slow down the motion of their faster partners and ensure the electric neutrality of the photoexcited electron–hole system.

where, considering the steady state conditions, we substituted the total derivative $\mathrm{d}/\mathrm{d}x$ for the derivative partial $\partial/\partial x$. Let us remind ourselves that τ is the (total) non-equilibrium carrier lifetime. When solving eqn (6.1) we apply the following boundary condition which tells us that the surface recombination described by the recombination rate S determines the value of the derivative of $n(x)$ at $x = 0$ according to relation

$$D \left.\frac{\mathrm{d}n(x)}{\mathrm{d}x}\right|_{x=0} = S\ n(x)\,|_{x=0}\,. \tag{6.2}$$

Note that S is expressed, as follows from (6.2), in cm/s.

An example of the solution of eqn (6.1) using the boundary condition (6.2) is graphically demonstrated in Figs 6.2(b) and (c). Panel (b) shows a strongly inhomogeneous photoexcitation profile $G = \alpha I_0 \exp(-\alpha x)$ under the common case of one-photon excitation. The second boundary condition here reads $n(x \to \infty) = 0$. Panel (c) refers to the case of a constant excitation profile G = const connected with the second boundary condition $n(x \to \infty) = G\tau$. This may occur, e.g. under two-photon laser excitation or in electric injection in luminescent diodes. It is observed that in both cases a marked decrease of the concentration $n(x)$ close beneath the surface, indeed, occurs which may

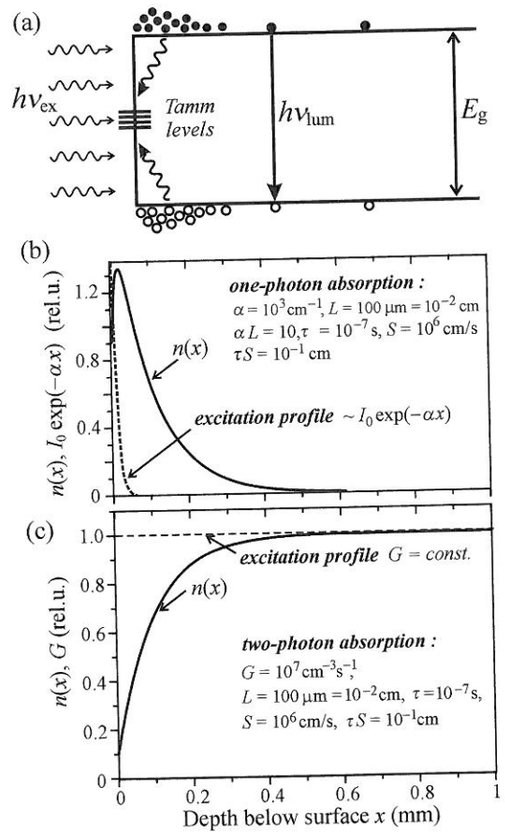

Fig. 6.2
Illustration of surface non-radiative recombination. (a) Schematic of photoexcitation and deep levels within the forbidden gap in the proximity of the surface. (b) Profiles of the generation rate $G(x) \sim I_0 \exp(-\alpha x)$ and of the excited carrier concentration $n(x)$ under one-photon excitation. (c) Carrier concentration profile $n(x)$ under a constant generation rate G = const (e.g. two-photon excitation). Parameters $L = (D\tau)^{1/2}$ (diffusion length), τ and S were chosen the same for both (b) and (c).

give rise to a luminescent 'dead layer' with strongly reduced luminescence intensity. The width of this layer can range—depending on the values of the parameters α, τ, S, D—from units to hundreds of micrometres. It should be mentioned that in order to demonstrate clearly the effects depicted in Figs6.2(b) and (c) a rather high surface recombination velocity ($S = 10^6$ cm/s) had to be chosen.

Under the condition G = const the subsurface decrease of $n(x)$ is more prominent and penetrates deeper. This fact can, on the one hand, be favourable in two-photon luminescence spectroscopy because it contributes to suppressing the spurious surface extrinsic radiative channels (Section 5.5). On the other hand, in applications—light-emitting semiconductor devices—the subsurface dead layer should be regarded as an undesirable effect which decreases the luminescence efficiency. In order to suppress the surface recombination special arrangements of the diode active layer are used. In general, the surface non-radiative recombination rate can be reduced by application of various passivation techniques which can decrease substantially the concentration of the subsurface recombination centres in the bandgap.

6.1.2 Auger and bimolecular recombination

Non-radiative Auger recombination in semiconductors can be considered parallel to the Auger effect known from electron spectroscopy of atoms and solids or from X-ray generation. In this process, an incident high-energy electron ejects another electron from an atomic core level; if some electron from an outer shell falls into the created vacancy, one X-ray photon is emitted. However, the filling process of the vacant state can also result in another outcome: the excitation energy is not released in the form of an emitted X-ray photon but, instead, is handed over to another electron from the same outer shell, ejecting it out of the atom. It is obviously a competing non-radiative process accompanying the X-ray generation.

As regards electron–hole pair recombination in semiconductors, an analogous Auger process is depicted in Fig. 6.3. It requires the presence of three quasi-particles, either two electrons and one hole (process *eeh*, see Fig. 6.3(a)) or two holes and one electron (process *ehh* from Fig. 6.3(b)). The energy released by one electron–hole pair recombination is transferred to the third quasi-particle which is then 'catapulted' either higher to the conduction band (e) or lower to the valence band (h). The energy of the recombining pair is passed to the third quasi-particle as its kinetic energy, and for this reason the Auger recombination is sometimes classified as an independent category of non-radiative transitions, characterized by the fact that the electronic excitation energy is—instead of being emitted as a luminescent photon—delivered to another electronic excitation. In the end, however, the kinetic energy of the third quasi-particle spills very rapidly (in picoseconds or their fractions) into the crystalline or amorphous matrix by multiphonon emission (Fig. 6.3, right column); the ultimate form of energy is therefore again heat. The ejected 'hot quasi-particle' (Auger quasi-particle) releases energy by relaxing to lower allowed energy levels in the respective band, taking advantage of the quasi-continuous character of these states.

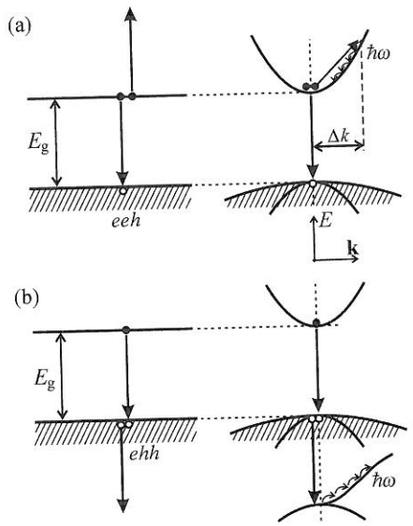

Fig. 6.3
Intrinsic non-radiative Auger recombination: (a) electron–electron–hole (*eeh*); (b) electron–hole–hole (*ehh*).

During the Auger process, obviously both energy and quasi-momentum conservation laws have to be satisfied. The schematics on the right-hand side of Fig. 6.3 show that the Auger process can occur both with (a) and without (b) involvement of a quasi-momentum conserving phonon $\hbar\Delta\mathbf{k}$; the no-phonon Auger process becomes feasible provided the ejected quasi-particle has to its disposal a suitable energy band, attainable without the alteration of wavevector of the (i.e. $\Delta\mathbf{k} = 0$). The latter alternative does not happen frequently; the first type of Auger process ($\Delta\mathbf{k} \neq 0$) is more common. The Auger mechanisms depicted in Fig. 6.3 can be called *intrinsic* because their occurrence is not conditioned by the presence of a defect or impurity.

Let us choose a rate of the non-radiative process $(\tau_{\mathrm{nr}}^{\mathrm{A}})^{-1}$ to be characteristic of the Auger recombination. Then we remember the bimolecular recombination described by eqn (3.9)

$$\frac{\mathrm{d}n(t)}{\mathrm{d}t} = G - \beta_{\mathrm{r}}\, n\, p - \beta_{\mathrm{nr}}\, n\, p, \tag{6.3}$$

where G is the generation term and $\beta_{\mathrm{r}}(\beta_{\mathrm{nr}})$ stands for the radiative (non-radiative) bimolecular recombination coefficient, see also Fig. 3.3. The Auger effect is a three-particle process, unlike two-particle recombination depicted in Fig. 3.3. We can therefore expect that Auger recombination will be described by a term $\sim np^2$ and instead of (6.3) it is possible to write

$$\frac{\mathrm{d}p(t)}{\mathrm{d}t} = G - A_{\mathrm{n}} n^2 p \qquad (eeh), \tag{6.4a}$$

$$\frac{\mathrm{d}n(t)}{\mathrm{d}t} = G - A_{\mathrm{p}} n\, p^2 \qquad (ehh), \tag{6.4b}$$

depending on whether the process (a) or (b) in Fig. 6.3 is under consideration. The so-called Auger coefficients A_{n}, A_{p} in eqn (6.4) will be related to the rate of non-radiative Auger recombination if we rewrite this equation in the form

$$\frac{\mathrm{d}p}{\mathrm{d}t} = G - \frac{p}{\tau_{\mathrm{nr}}^{A_{\mathrm{n}}}}, \tag{6.5a}$$

$$\frac{\mathrm{d}n}{\mathrm{d}t} = G - \frac{n}{\tau_{\mathrm{nr}}^{A_{\mathrm{p}}}}. \tag{6.5b}$$

By comparing eqns (6.4a), (6.4b) with (6.5a), (6.5b) we obtain

$$\frac{1}{\tau_{\mathrm{nr}}^{A_{\mathrm{n}}}} = A_{\mathrm{n}}\, n^2, \qquad \frac{1}{\tau_{\mathrm{nr}}^{A_{\mathrm{p}}}} = A_{\mathrm{p}}\, p^2. \tag{6.6}$$

Typical values of the Auger coefficient in semiconductors are of the order of $A \sim 10^{-31}$–$10^{-29}\mathrm{cm}^6/\mathrm{s}$, exceptionally (for the no-phonon process $\Delta\mathbf{k} = 0$) up to $10^{-26}\mathrm{cm}^6/\mathrm{s}$. The quadratic dependence of $(\tau_{\mathrm{nr}}^{A})^{-1}$ on the carrier concentration in eqn (6.6) signifies an important fact: the intrinsic Auger effect occurs mainly for high concentrations of free carriers. The (*eeh*) is type is expected to be found mainly in n-type semiconductors, while (*ehh*) is predominantly in p-type materials. Non-radiative Auger recombination obviously plays an important role in luminescence processes under high excitation and also whenever multiple free electron–hole pairs are localized in a small volume, e.g. in nanocrystals. Auger lifetimes τ_{nr}^{A} for n, $p = 10^{18}\mathrm{cm}^{-3}$ are of the order of 10^{-6} s, but for n, $p = 10^{19}\mathrm{cm}^{-3}$ they drop to only 10^{-8} s (!). It is worth noting that intrinsic Auger recombination contributes to the fact that luminescence of narrow-bandgap semiconductors is weak. The reason is that easy thermal generation of free carriers across the bandgap leads to a relatively high free carrier concentration already in unexcited material.

In addition to intrinsic Auger recombination, there also exists *extrinsic Auger recombination* when carriers localized at impurities also play a role. An example of such a process is displayed in Fig. 6.4: a non-radiative process accompanying luminescence originating in the transitions (e–A^0) and (h–D^0) and therefore decreasing its efficiency. Again a high concentration of free carriers or impurity atoms is essential here because the interaction of, for example, a free electron with an electron localized on a donor must occur, which is conditioned by the close proximity to each other. A slightly different type of extrinsic Auger process (accompanying bound exciton recombination) will be discussed in Chapter 7.

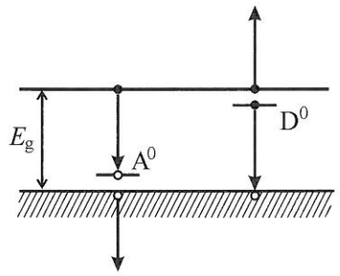

Fig. 6.4
Extrinsic nonradiative Auger recombination competing with radiative transitions ($e - \mathrm{A}^0$) and ($h - \mathrm{D}^0$). Compare with Fig. 5.7.

Let us now return to the question of non-radiative bimolecular recombination of free carriers. We know that bimolecular recombination, both radiative and non-radiative, is characterized by the quadratic nature of the recombination terms in kinetic equations of the type (6.3) or (3.9). We have already noted that the probability of such non-radiative processes in an ideal pure semiconductor (Fig. 6.1(a)) is in fact zero. In spite of this, it has been discovered experimentally that bimolecular non-radiative recombination occurs in a wide range of materials. We will show that the reason for this may lie in the existence of strongly localized states approximately in the middle of the bandgap (a suitably located 'deep level') and their co-actions with Auger recombination. (One therefore deals with the extrinsic effect because deep levels are due either to a defect or an impurity.) This mechanism has been proposed by Juška *et al.* [3].

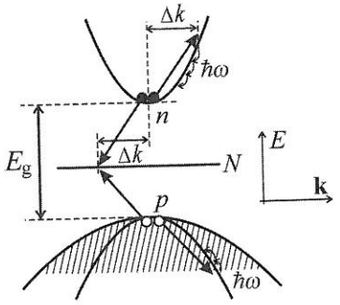

Fig. 6.5
Bimolecular nonradiative recombination mediated by a deep level (with concentration N) in the forbidden band in cooperation with Auger recombination of electrons (n) and holes (p) in respective extremes of the valence and conduction bands. $\hbar\Delta\mathbf{k}$ stands for quasi-momentum change, $\hbar\omega$ is phonon energy.

The process is clarified by the schematic sketch in Fig. 6.5. Its basis consists in Auger recombination of free electrons and holes in relevant bands; however, the final state of the transition of the particle releasing energy becomes the deep level within the forbidden gap. At the same time, if this energy state is strongly localized in **r**-space, it is strongly delocalized in **k**-space, which facilitates automatic satisfaction of the quasi-momentum conservation law. The probability of such processes is therefore high. Furthermore, its rate in comparison with the Auger recombination across the full bandgap (Fig. 6.3) is enhanced because of the smaller required change $\Delta\mathbf{k}$ in the Auger particle wavevector (for the Auger recombination matrix element M_A we have $M_A \approx 1/(\Delta\mathbf{k})^2$).

Let N be the concentration of the localized states, $n = p$ the concentration of the excited free carriers and n_N the momentary concentration of electrons on the localized level; the corresponding kinetic equations for electrons read

$$\frac{dn}{dt} = -A_n n^2 (N - n_N) \tag{6.7}$$

and for holes

$$\frac{dp}{dt} = -A_p p^2 n_N = -A_p n^2 n_N.$$

We eliminate n_N:

$$\frac{dn}{dt} = -A_n n^2 N - \frac{A_n}{A_p}\frac{dn}{dt},$$

$$\frac{dn}{dt}\left(1 + \frac{A_n}{A_p}\right) = -(A_n N) n^2,$$

$$\frac{dn}{dt} = -\left[\frac{A_n N}{(1 + A_n/A_p)}\right] n^2 = -\beta_{nr} n^2. \tag{6.8}$$

Therefore, the process depicted in Fig. 6.5 indeed has a bimolecular character, as reflected in the quadratic dependence $\sim n^2$. If $A_n = A_p = 10^{-27}\text{cm}^6/\text{s}$ ($\Sigma\Delta\mathbf{k} = 0$, the Auger coefficients therefore have high values) and $N = 10^{18}\text{cm}^{-3}$, we get from (6.8) for the bimolecular coefficient of non-radiative recombination $\beta_{nr} = 5 \times 10^{-10}\,\text{cm}^3/\text{s}$, a value in order-of-magnitude agreement with both experiment and the typical magnitude of the radiative bimolecular coefficient β_r, see Section 3.3.

Let us emphasize that the effective functioning of this model assumes a relatively high concentration of the deep traps, because there has to be a positive value $(N - n_N)$ on the right side of eqn (6.7). This model was originally proposed for amorphous silicon where the role of the deep levels is played by valence band tail states, which fulfil the above condition. Also a relatively high excitation is indispensable because it is in principle necessary to fulfil another condition n, $p > N$ in order to ensure a sufficient concentration of electrons and holes in the extremes of the bands during rapid carrier capture in the deep trap.

6.2 Creation of lattice defects

The principle of this excitation energy dissipation lies in the following mechanism: An electronic excitation is localized at some atom occupying a regular lattice position. Relaxation of such an excited atom into the ground state can proceed in the following way: the released excitation energy is transferred to the relevant atom as a whole, which is thus 'kicked off' into an interstitial lattice position, creating a so-called Frenkel defect (a vacancy plus an interstitial atom). This defect can be either transient or permanent depending on whether the interstitial atom does or does not return into its original lattice site once the excitation is terminated.

In order to make this non-radiative recombination process possible, the following criteria must be fulfilled, [4]:

(a) *Localization of the electronic excitation* must occur. Expressed quantitatively, the lifetime of such an excitation at the atom in question must be higher than the effective vibration period of the lattice, because the creation of the Frenkel defect is conditioned by relatively slow displacements of surrounding heavy atoms or ions. Strong localization of the excitation happens most easily if photoexcited electrons and holes or excitons move slowly throughout the crystal lattice. This occurs most probably when they have high effective masses, thus *polarons* with non-zero coupling constants α_e, α_h (Table 4.2) appear to be good candidates. It can be shown that the polaron mass m_p^* is connected with the effective mass of a 'bare' quasi-particle m^* by the expression

$$m_p^* = \frac{1 - 0.08\alpha^2}{1 - \alpha/6 + 0.0034\,\alpha^2}\, m^* \approx \left(1 + \frac{\alpha}{6}\right) m^*, \tag{6.9}$$

therefore $m_p^* > m^*$(the approximation on the right side holds for $\alpha \leq 0.5$). Such a localized excitation is usually called a self-trapped exciton; we will address self-trapped excitons in the next chapter.

One can immediately infer from Table 4.2 that the creation of self-trapped excitons is to be expected in II–VI and I–VII semiconductors, which have considerable ionic binding, a strong exciton–phonon interaction and a relatively wide forbidden gap.

(b) *Energy criterion*. The energy of the self-trapped exciton E_e (which does not differ too much from the bandgap width E_g) must of course be higher than the energy E_d of formation of the defect

$$E_g \geq E_e > E_d. \tag{6.10}$$

The energy E_d required by an atom or ion to jump to an interstitial position is very weakly dependent on the type of semiconductor and is mostly in the range of 1.5–3.5 eV. Relation (6.10) tells us, in accordance with criterion (a), that the creation of a lattice defect is mainly a feature of wide-bandgap semiconductors with a high fraction of ionic binding.

(c) *Protection against degradation to heat—phonons*. Local vibrations in the vicinity of an atom around which the self-trapped exciton gets localized

must have a frequency ω_ℓ higher than the highest LO-phonon frequency $\omega_{\max}^{\mathrm{LO}}$, i.e. $\omega_\ell > \omega_{\max}^{\mathrm{LO}}$, which guarantees that phonons do not 'spread' the localized energy over the whole crystal. The phonon mode concerned must thus belong, referring to Fig. 4.7(d), among the so-called local modes, resulting from an increase of the effective spring constant $f = M\,\omega_\ell^2$ around the localized excitation; redistribution of the charge density accompanied by changes of the equilibrium atom positions may indeed often lead to the required increase of f.

(d) *Orientation criterion.* The self-trapped exciton (its charge density) should have a suitable symmetry in the crystal lattice so that the creation of the interstitial atom is energetically favourable.

An example of a semiconductor material in which such defect formation owing to the localized electronic excitation very probably occurs is AgCl. Here, the exciton–phonon interaction is so strong that a self-trapped exciton (in the form of an autolocalized hole on a silver ion $(AgCl_6)^{4-}$ in the lattice, which subsequently attracts a photoelectron via Coulomb interaction) is created at low temperatures very rapidly (in the order of picoseconds). In addition to radiative recombination, presenting itself as a broadband blue-green luminescence, this localized exciton can recombine also non-radiatively causing the relevant Ag^+ ion to be pushed out (probably only transiently) into an interstitial position. Therefore a Frenkel defect is created.

Interstitial silver ions Ag^+ in silver halides can also be created by heating; these materials are characterized by a rather high concentration of these interstitial ions, about 10^{13}–$10^{14}\,\mathrm{cm}^{-3}$ at room temperature. Their presence, hand in hand with their mobility, plays a fundamental role in photolysis and the formation of latent photographic images.

6.3 Photochemical changes

In silver halides AgCl, AgBr and AgI at sufficiently high temperatures ($T \geq 200\,\mathrm{K}$) there exists, besides defect formation, another channel dissipating energy of the optically created electron–hole pairs. A photoelectron becomes captured at a certain 'photosensitivity centre' while a hole gets localized on a Cl^- ion. The captured electron then attracts an interstitial Ag^+ ion which is able to diffuse rather freely through the lattice (the diffusion coefficient of the Ag^+ ions at room temperature is of the order of $10^{-12}\,\mathrm{cm}^2/\mathrm{s}$, while that of Cl^- ions is by several orders lower, basically unmeasurable). A neutral Ag^0 atom results, and successive trapping of other electrons and Ag^+ ions may lead to the growth of a metallic silver cluster—a seed of the latent photographic image:

$$\mathrm{Ag}^+ \underset{e}{\rightarrow} \mathrm{Ag}^0 \underset{e}{\rightarrow} \mathrm{Ag}^- \underset{\mathrm{Ag}^+}{\rightarrow} 2\mathrm{Ag}^0 \underset{\mathrm{Ag}^+}{\rightarrow} 3\mathrm{Ag}^+ \underset{e}{\rightarrow} 3\mathrm{Ag}^0 \underset{e}{\rightarrow} 3\mathrm{Ag}^- \ldots \qquad (6.11)$$

Sufficient mobility both of the electrons and of the interstitial metal ions, Ag^+ (the specificity of silver halides resides just in this) is therefore essential, and also a sufficiently high temperature is required because the ion mobility grows exponentially with T. The captured holes neutralize the Cl^- ions and chlorine

gas leaks out, at least from the surface layers of the crystal. Therefore, a photochemical dissociation of the solid occurs.

At low temperatures ($T \leq 100\,\mathrm{K}$) the motion of the interstitial Ag^+ obviously becomes strongly limited ('freezes'), the formation of the latent image fades away and silver halides become, on the contrary, relatively efficient phosphors. Their properties under UV irradiation are then very stable. (Hardly anybody is aware of the impossibility of taking photographs at cryogenic temperatures.) There exists a rather wide range of temperatures (100–200 K) where all three actions, i.e. radiative recombination, defect formation and photochemical reaction, may coexist. It is interesting that, although silver halides have been widely used in photography for as long as 150 years, a detailed understanding of all the steps in the reaction described by scheme (6.11) is still lacking. In particular, what is not fully clear is the microscopic nature of the primary photosensitivity centres.

Similar photographic processes occur, nevertheless with much lower efficiency, in halides of lead ($PbCl_2$), thallium (TlCl, TlBr) and mercury (Hg_2Cl_2, Hg_2Br_2); all these materials show luminescence in the visible region at low temperatures.

6.4 Problems

6/1: If a bimolecular radiative recombination $\sim \beta n^2$ and Auger non-radiative recombination $\sim An^3$ are simultaneously active in a semiconductor, the non-equilibrium carrier concentration $n(= p)$ is driven by the kinetic equation

$$\frac{\mathrm{d}n}{\mathrm{d}t} = -\beta\, n^2 - A\, n^3.$$

In the case when non-radiative recombination prevails (i.e. $\beta \ll An$), it will be possible to detect a very weak luminescence, whose kinetic behaviour will be described by the equation $\mathrm{d}n/\mathrm{d}t \cong -An^3$. Show that the luminescence decay curve can then be expressed as $I(t) = I(0)/[1 + 2AI(0)t/\beta]$, where $I(0) = \beta n^2(0)$ is the intensity at time $t = 0$.

6/2: *Quick graphical test of the type of recombination mechanism.* From the experimentally measured curve of a luminescence decay $I(t)$ (Fig. 6.6) it is possible to deduce the dominating type of carrier recombination by making use of the following method: We plot the curve on a semi-logarithmic scale and at several points we draw a tangent, thereby obtaining several values of its slope $\tan\alpha$. Then we plot $\ln|\tan\alpha|$ as a function of $\ln I(t)$. If this plot is constant, independent of $I(t)$, the dominating recombination is monomolecular, if it constitutes a straight line with slope 1/2 then a bimolecular recombination dominates, and a straight line with slope 1 indicates that non-radiative Auger recombination prevails. Prove this. (Hint: Start from the explicit expressions for $I(t)$. Employ the results of Problem 6/1.)

6/3: Discuss the experimental methods applied to study the Auger effect in semiconductors according to [2]; see also [5].

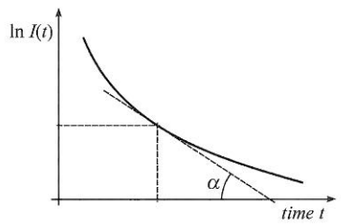

Fig. 6.6

References

1. Abakumov, V. N., Perel, V. I., and Yassievich, I. N. (1991). *Nonradiative recombination in semiconductors*. In *Modern Problems in Condensed Matter Sciences*, Vol. 33 (ed. V. M. Agranovich and A. A. Maradudin). North Holland, Amsterdam.
2. Pilkuhn, M. H. (1981). *Light emitting diodes*. In *Handbook on Semiconductors* (ed. T. S. Moss), Vol. 4 (ed. C. Hilsum), p. 539. North Holland, Amsterdam.
3. Juška, G., Viliunas, M., Arlauskas, K., and Kočka, J. (1995-I). *Phys. Rev. B*, **51**, 16668.
4. Luščik, Č. B. and Luščik, A. Č. (1989). *Decay of electronic excitations with defect formation in solids* (in Russian: *Raspad elektronnych vozbuždënij s obrazovaniem defektov v tverdych telach*). Nauka, Moskva.
5. Dziewior, J. and Schmid, W. (1977). *Appl. Phys. Lett.*, **31**, 346; Benz, G. and Conradt, R. (1977). *Phys. Rev. B*, **16**, 843.

Luminescence of excitons

7

In an ideal pure semiconductor, the primary electronic excitation is a free electron–hole pair, the energy required for its creation (supplied, for example, by an incident photon) being equal—at the very minimum—to the bandgap value E_g. In a simplified way, an exciton may be visualized as a couple consisting of an electron and the associated hole, attracted to each other via Coulomb forces. Therefore, such a bound electron–hole pair no longer represents two independent quasi-particles and its internal energy is lower than E_g. The exciton is thus a quasi-particle representing the lowest electronic excitation in a semiconductor. There exist three basic types of excitons:

1. *Frenkel exciton* or a small-radius exciton. The spatial extension of the excitation is approximately restricted to a single unit cell. These excitons are to a large extent localized at a specific atom or molecule, and their movement through the crystal is limited to a hopping mechanism. They occur in molecular crystals.
2. *A charge transfer exciton* occurs primarily in ionic crystals. One can imagine its creation as follows: An electron is transferred from a lattice anion to a nearest neighbour cation, thereby creating there a maximum of the electron charge density. The radius of the charge transfer exciton can therefore be somewhat larger than that of the Frenkel exciton.
3. *Wannier exciton* or a large-radius exciton. The electron and hole are separated over many lattice constants, the exciton wavefunction is strongly delocalized and the exciton can move freely inside the crystal. Such a quasi-particle is also called a *free exciton*. The free exciton transfers the excitation energy, however, not the electric charge, because—as a whole—it is electrically neutral. Wannier excitons occur mainly in semiconductors.

The annihilation of an exciton is accompanied by a characteristic luminescence due to radiative recombination of the electron with the hole. In this chapter, we shall explain in detail the concept of the Wannier exciton and expound how it manifests itself in luminescence. Afterwards, we shall discuss the characteristic features of luminescence of the so-called bound excitons (i.e. excitons localized at impurity atoms or self-trapped owing to the strong exciton–phonon interaction).